

Scanning Tunneling Spectroscopic Studies of the Pairing State of Cuprate Superconductors

N.-C. Yeh, C.-T. Chen, R. P. Vasquez*, C. U. Jung[†], S.-I. Lee[†],
K. Yoshida[‡] and S. Tajima[‡]

*Department of Physics, California Institute of Technology, Pasadena,
CA 91125, USA*

**Jet Propulsion Laboratory, California Institute of Technology, Pasadena,
CA 91109, USA*

*[†]Department of Physics, Pohang University of Science and Technology,
Pohang 790-784, Korea*

*[‡]Superconductivity Research Laboratory, International Superconductivity
Technology Center, Sinonome, Koto-ku, Tokyo, 135 Japan*

Quasiparticle tunneling spectra of both hole-doped (p-type) and electron-doped (n-type) cuprates are studied using a low-temperature scanning tunneling microscope. The results reveal that neither the pairing symmetry nor the pseudogap phenomenon is universal among all cuprates, and that the response of n-type cuprates to quantum impurities is drastically different from that of the p-type cuprates. The only ubiquitous features among all cuprates appear to be the strong electronic correlation and the nearest-neighbor antiferromagnetic Cu^{2+} - Cu^{2+} coupling in the CuO_2 planes.

PACS numbers: 74.72.-h, 74.50.+r, 74.62.Dh

1. INTRODUCTION

To date there has been no consensus for the mechanism of cuprate superconductivity. The diverging views are primarily due to complications incurred by competing orders in these strongly correlated doped Mott insulators.^{1,2,3} The competing orders can result in a variety of phases in the ground state, depending on whether the cuprate is hole doped (p-type) or electron doped (n-type), and also on the carrier doping level, the electronic coupling strength between neighboring CuO_2 planes, and the degree of disorder.^{4,5,6,7} In order to sort through the complications, it is necessary

to identify universal characteristics among all cuprate superconductors.

Among the noteworthy phenomena associated with the cuprates, $d_{x^2-y^2}$ -wave pairing symmetry,^{8,9} spin fluctuations,¹⁰ pseudogap phenomenon,¹¹ strong phase fluctuations¹² and stripe phases¹³ have been considered as important to the underlying mechanism. In particular, the pseudogap phenomenon is widely regarded as a precursor to superconductivity, and its doping dependence together with the non-Fermi liquid behavior in the pseudogap regime have led to the hypothesis for a quantum critical point (QCP) near the optimal doping level¹⁴ as well as other models such as preformed Cooper pairs,¹⁵ Bose-Einstein condensation at T_c ,¹⁶ $d_{x^2-y^2}$ -density wave phase with orbital currents in the pseudogap regime,¹⁷ and spin gap scenario.¹⁸ However, these models have been developed around experimental findings in the p-type cuprates. Given that the cuprates cannot be properly described by a simple one-band Hubbard model and therefore lack apparent particle-hole symmetry, it is not obvious whether all phenomena in the p-type cuprates can be generalized to the n-type cuprates.

In this work, we compare the quasiparticle tunneling spectra of a variety of p-type and n-type cuprate superconductors, with special emphasis on the doping dependence and the effects of quantum impurities in the CuO_2 planes. The physical implications of our investigation are discussed.

2. PAIRING STATE OF THE P-TYPE CUPRATES

The p-type cuprates studied in this work include the under- and optimally doped $\text{YBa}_2\text{Cu}_3\text{O}_{7-\delta}$ (YBCO), overdoped YBCO with Ca-substitution, an optimally doped YBCO with 0.26% Zn and 0.4% Mg substitutions for Cu in the CuO_2 planes,^{4,5,6} and the under- and optimally doped $\text{La}_{2-x}\text{Sr}_x\text{CuO}_{4-\delta}$ (LSCO) system.¹⁹ The spectra are taken using a low-temperature scanning tunneling microscope (STM), with the average quasiparticle momentum along different crystalline axes. The surface preparation with chemical etching method and surface characterizations are described elsewhere.^{4,20,21}

2.1. Doping-Dependent Pairing Symmetry and Pairing Potential

The pairing symmetry and momentum (k)-dependent pairing potential Δ_k can be derived self-consistently by applying the generalized BTK analysis to the directional tunneling spectra taken on each sample.^{4,5,22} We find that the pairing symmetry of p-type cuprates is dependent on the doping level and the crystalline structure. For cuprates with orthorhombic structure such as the YBCO system, the pairing symmetry is predominantly $d_{x^2-y^2}$ -wave in

Scanning Tunneling Spectroscopic Studies of Cuprate Superconductors

the underdoped regime and ($d_{x^2-y^2} + s$)-wave with a significant s -wave component increasing with doping in the overdoped limit.^{4,5,6} On the other hand, for tetragonal samples such as the $\text{Bi}_2\text{Sr}_2\text{CaCu}_2\text{O}_x$ (BSCCO) and LSCO, the pairing symmetry is consistent with pure $d_{x^2-y^2}$ -wave for all doping levels. Moreover, no discernible complex order parameter could be detected in the p-type cuprates based on our STS studies.^{4,5,6} Therefore no obvious QCP with a universal broken symmetry can be identified in the p-type cuprates based on our tunneling studies. In addition, the $d_{x^2-y^2}$ -component of the superconducting gap (Δ_d) in the YBCO system is only weakly dependent on the doping level for the optimal and underdoped samples,^{4,5,6} and is reduced significantly in the overdoped regime, as shown in Fig. 1(a). These gap values do not persist above T_c ,²³ and are therefore consistent with the pairing potential. Our findings are in contrast to the point-contact spectra of BSCCO that exhibit a rapidly increasing averaged energy gap with decreasing doping,²⁴ and the large averaged gap of the underdoped BSCCO appears to merge with the pseudogap. However, recent tunneling experiments on BSCCO mesas suggest that the spectral pseudogap does not have the same physical origin as the superconducting gap.²⁵ We also note that the $(2\Delta_d/k_B T_c)$ ratio in YBCO increases with decreasing doping level, suggesting increasing electronic correlation in the underdoped regime.^{4,5,6}

In general, the quasiparticle spectra of the YBCO system exhibit long-range spatial homogeneity for most doping levels,^{4,5} in contrast to the nano-scale spectral variations found in some underdoped BSCCO.²⁶ This difference may be attributed to the more homogeneous oxygen distribution in YBCO, where oxygen vacancies exist in the CuO-chains and are often structurally ordered. In contrast, oxygen vacancies in BSCCO can exist in different atomic planes and are generally disordered, thereby giving rise to nano-scale inhomogeneity in underdoped BSCCO. From the perspective of competing orders, nano-scale phase separations can occur for limited doping levels. Indeed, significantly more homogeneous tunneling gap values have been reported for tunneling directly into the CuO_2 plane of a BSCCO sample,²⁷ implying that nano-scale phase separations need not be a natural consequence of short superconducting coherence lengths.

2.2. Effects of Quantum Impurities

An important consequence of either $d_{x^2-y^2}$ or ($d_{x^2-y^2} + s$) pairing symmetry is the existence of low-energy nodal quasiparticle excitations. These fermionic excitations can interact strongly with quantum impurities in the CuO_2 plane and significantly influence the local quasiparticle spectra near

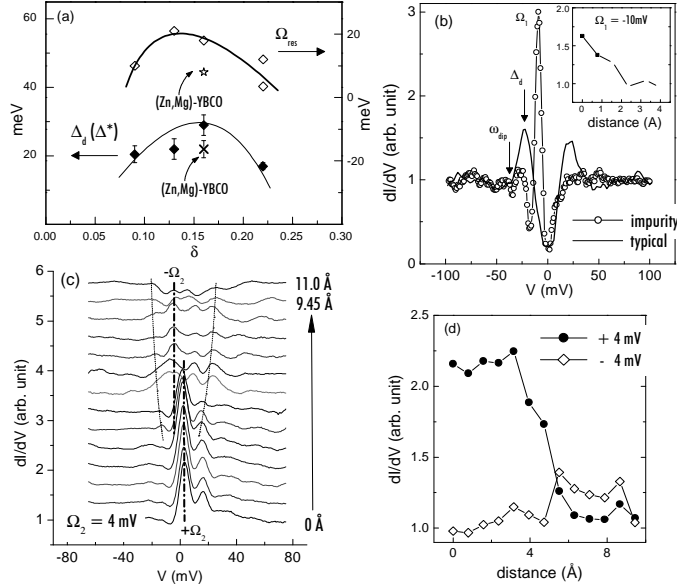


Fig. 1. (a) Doping dependent pairing potential Δ_d and spin excitation energy Ω_{res} of YBCO. (b) c -axis tunneling spectra of a YBCO single crystal at and far away from a non-magnetic impurity with a resonant scattering peak at $\Omega_1 \approx -10meV$. (c) Spatial evolution of the c -axis tunneling spectra near a non-magnetic impurity with a scattering peak at $\Omega_2 \approx +4meV$. (d) Spatial evolution of the differential conductance in (c) at $\pm\Omega_2$. All spectra were taken at 4.2 K.

impurities.^{28,29,30,31} Furthermore, the existence of nearest-neighbor antiferromagnetic $Cu^{2+}-Cu^{2+}$ correlation in the superconducting state can induce effective Kondo-like magnetic moments on the neighboring Cu^{2+} ions of a spinless impurity (such as Zn^{2+} , Mg^{2+} , Al^{3+} and Li^+ with $S = 0$),³² as confirmed from nuclear magnetic resonance (NMR)^{33,34} and inelastic neutron scattering (INS)³⁵ experiments. These strong effects in the p-type cuprates are in contrast to the insensitivity of conventional superconductors to spinless impurities³⁶.

Most theoretical studies of the quasiparticle tunneling spectra near quantum impurities are restricted to perturbative and one-band approximation^{28,29,30,31,32}. The Hamiltonian (\mathcal{H}) is approximated by $\mathcal{H} = \mathcal{H}_{BCS} + \mathcal{H}_{imp}$, where \mathcal{H}_{BCS} is the d -wave BCS Hamiltonian and \mathcal{H}_{imp} due to impurities contains both the potential scattering term \mathcal{H}_{pot} and the magnetic exchange term \mathcal{H}_{mag} :³²

$$\mathcal{H}_{imp} = \mathcal{H}_{pot} + \mathcal{H}_{mag} = U \sum_{\sigma} c_{0\sigma}^{\dagger} c_{0\sigma} + \sum_{\vec{R}} J_{\vec{R}} \mathbf{S} \cdot \sigma_{\vec{R}}. \quad (1)$$

Scanning Tunneling Spectroscopic Studies of Cuprate Superconductors

Here U is the on-site Coulomb scattering potential, c^\dagger and c are particle operators, and $J_{\vec{R}}$ is the exchange coupling constant between the spin of conduction carriers on the \vec{R} sites and the localized magnetic moment (S). If one further neglects variations in the tunneling matrix and assumes a pure potential scattering contribution, one obtains a resonant energy at Ω_0 on the impurity site using Eq. (1):^{28,29,30}

$$|\Omega_0/\Delta_d| = (\pi/2) \cot \delta_0 \ln (8/\pi \cot \delta_0), \quad (2)$$

where δ_0 is the impurity-induced phase shift in the quasiparticle wavefunction. On the other hand, for point-like magnetic impurities with exchange interaction limited to the s -channel, one obtains two spin-polarized impurity states at energies $\Omega_{1,2}$:³¹

$$|\Omega_{1,2}/\Delta_d| = 1/[2\mathcal{N}_F(U \pm W) \ln |8\mathcal{N}_F(U \pm W)|], \quad (3)$$

where \mathcal{N}_F is the density of states at the Fermi level and $W \equiv \mathbf{J}\mathbf{S} \cdot \boldsymbol{\sigma}$ assumes isolated and equivalent magnetic impurities at all sites. In contrast, for *induced* magnetic moments on the neighboring Cu^{2+} sites due to a spinless impurity, the perturbation Hamiltonian \mathcal{H}_{mag} must include the four Cu sites \vec{R} adjacent to the impurity with $J_{\vec{R}} = J/4$ and also involve screening channels associated with s -, p_x -, p_y - and d -wave like conduction electrons on the four sites.³² The resulting quasiparticle spectra exhibit a single resonant peak at the impurity site and alternating intensities and signs of the peak energy away from the impurity.³²

We have performed STS studies on an optimally doped YBCO with 0.26% Zn and 0.4% Mg substitution. The T_c of this sample is 82 K, substantially lower than that of optimally doped YBCO ($T_c = 93$ K). The representative spectroscopic information is illustrated in Figs. 1(b)–(d). For STM tip significantly far away from any impurities, the tunneling spectra are similar to typical c -axis quasiparticle tunneling spectra in pure YBCO, although the global superconducting gap Δ_d is suppressed to (25 ± 2) eV from the value $\Delta_d = (29 \pm 1)$ meV in pure YBCO, as shown in Fig. 1(a).^{4,5} Moreover, the energy ω_{dip} associated with the “dip-hump” satellite features also shifts substantially relative to that in pure YBCO. The dip-hump features have been attributed to quasiparticle damping by many-body excitations such as spin fluctuations or phonons,^{37,38,39} and the resonant energy of the many-body excitation can be empirically determined via $|\Omega_{res}| = |\omega_{dip} - \Delta_d|$. We find that $|\Omega_{res}|$ decreases significantly to (7 ± 1) meV from the value (17 ± 1) meV in pure YBCO. This drastic decrease suggests that phonons are unlikely the relevant many-body excitations that contribute to the satellite features. On the other hand, the local spectral evolution suggests that there are two types

of impurities, one with a resonant scattering energy $\Omega_1 \sim -10$ meV and the other with $\Omega_2 \sim 4$ meV at the impurity site.^{4,5} The intensity of the resonant peak decreases rapidly within approximately one Fermi wavelength along the Cu-O bonding direction, as shown in the insets of Figs. 1(b) and (c). Moreover, the resonant scattering peak appears to alternate between energies of the same magnitude and opposite signs as the STM tip is displaced away from an impurity, as exemplified in Fig. 1(c). Some of these spatially varying spectra near impurities even reveal slow temporal variations over long times (about $\sim 10^2$ s). Although more detailed studies and proper consideration of the tunneling matrix^{40,32} are needed to fully understand the relative contributions of \mathcal{H}_{pot} and \mathcal{H}_{mag} , the presence of temporal variations might be more consistent with the Kondo effect. For comparison with other systems, however, we may assume pure potential scattering and use Eq. (2) to derive the corresponding phase shifts associated with the spinless quantum impurities. We obtain $\delta_1 \sim 0.38\pi$ and $\delta_2 \sim 0.43\pi$ in comparison with the phase shift ($\delta_0 \sim 0.45\pi$) due to Zn in BSCCO⁴¹, suggesting that the impurity scattering strength in YBCO is weaker.

3. PAIRING STATE OF THE N-TYPE CUPRATES

Despite strong consensus for the pairing symmetry in p-type cuprates as being predominantly $d_{x^2-y^2}$,^{8,9} the situation associated with the n-type cuprates remains controversial. In the case of one-layer n-type cuprates $\text{Ln}_{2-x}\text{M}_x\text{CuO}_4$ system (Ln = Nd, Sm, Pr; M = Ce, Sr), tunneling spectroscopic studies on bulk materials are consistent with *s*-wave pairing⁴² whereas phase sensitive measurements on thin films suggest $d_{x^2-y^2}$ -pairing.⁴³ Recently, further studies of the one-layer n-type cuprates have implied doping dependent pairing symmetry.⁴⁴

3.1. Strongly Correlated S-Wave Pairing

Our STS studies of the simplest form of cuprate superconductors, the n-type “infinite-layer” system $\text{Sr}_{0.9}\text{La}_{0.1}\text{CuO}_2$ (SLCO) with $T_c = 43$ K⁴⁶ reveal momentum-independent quasiparticle tunneling spectra, as manifested by consistent spectral characteristics among data taken on more than 300 randomly oriented grains of a polycrystalline SLCO sample.^{6,7} A representative spectrum is shown in Fig. 2(a). This finding together with the absence of any *d*-wave spectral characteristics (see Fig. 2(b) with $\Delta_k = \Delta_d(k_x^2 - k_y^2)$) is suggestive of *s*-wave pairing symmetry.⁷ To further investigate the possibility of any anisotropy, we use the generalized BTK analysis to derive

Scanning Tunneling Spectroscopic Studies of Cuprate Superconductors

tunneling spectra for the anisotropic pairing potentials permitted by symmetry. For the D_{4h} point group associated with the infinite-layer system, we may consider the lowest energy configurations in the pairing state with angular momenta $\ell = 0, 2, 4$. We find that the pairing potential of the A_{1g} representation and $\ell = 0$ corresponds to the isotropic s -wave pairing potential Δ_0 , and that ℓ up to 2 is given by $\Delta_k = \Delta_{xy}(k_x^2 + k_y^2) + \Delta_z k_z^2$, where Δ_{xy} and Δ_z are the in-plane and c -axis pairing potentials. For ℓ up to 4, two pairing potentials of the A_{1g} representation are possible. One is similar to that for $\ell = 2$ with uniaxial symmetry, the other exhibits four-fold modulations in the k_x - k_y plane, with $\Delta_k = \Delta_0 + \Delta_1(k_x^4 + k_y^4 - 6k_x^2 k_y^2)$. The tunneling spectra for these possibilities are shown in Figs. 2(c) and (d), which suggest that all pairing potentials with anisotropy would have resulted in significantly varying tunneling gap values with the quasiparticle momenta. Comparing this analysis with our data and experimental resolution, we estimate $\sim 8\%$ upper bound for any anisotropy in the pairing potential.

The finding of s -wave pairing symmetry may be related to the fact that the n -type infinite-layer system is the only cuprate with a c -axis superconducting coherence length longer than the c -axis lattice constant.^{7,46,49} This unique property is in contrast to the quasi-two dimensional superconductivity in all other cuprates. Additional noteworthy phenomena include insignificant satellite features, which imply much reduced spin fluctuations below T_c , and the absence of pseudogap above T_c , as shown in Fig. 2(a). The insignificant spin fluctuations are consistent with the fact that electron doping results in formation of Cu^+ -ions that dilute the antiferromagnetic Cu^{2+} - Cu^{2+} correlation without causing significant spin fluctuations as holes do in the oxygen p -orbitals, and the absence of pseudogap above T_c is also consistent with similar findings in the one-layer n -type cuprates.⁴⁸

3.2. Effects of Quantum Impurities

In contrast to the sensitive response of p -type cuprates to both magnetic and non-magnetic impurities, the response of the infinite-layer system appear to be more consistent with that in conventional superconductors.^{36,45,47} That is, little suppression in either T_c or the superconducting gap is found with Zn^{2+} -impurity substitution up to 3%.^{49,7} In contrast, strong T_c suppression and significant impurity-induced electron-hole asymmetry in the quasiparticle spectra were found with small concentrations of Ni^{2+} -impurities.^{49,7} Moreover, our studies of the local quasiparticle density of states in the 1% Ni -substituted SLCO sample reveal long-range impurity effects, with strong particle-hole asymmetry due to the magnetic impurity-induced broken time-

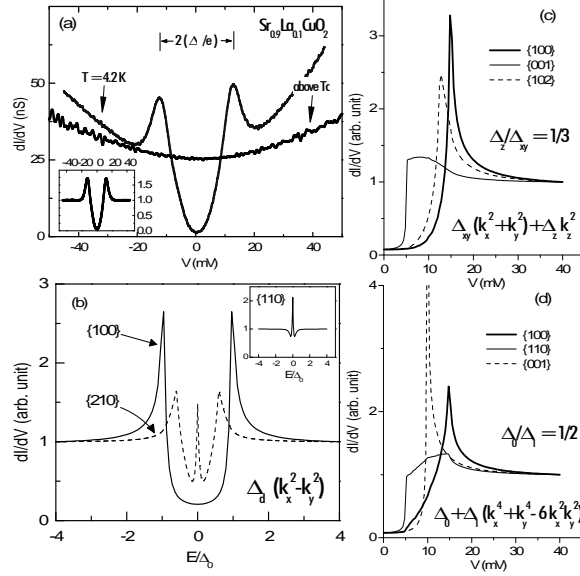


Fig. 2. (a) Normalized momentum-independent quasiparticle tunneling spectra in a pure $\text{Sr}_{0.9}\text{La}_{0.1}\text{CuO}_2$ taken at $T = 4.2$ K. (b) Calculated spectra for quasiparticle tunneling along different crystalline axes of a pure $d_{x^2-y^2}$ -wave superconductor. (c) Calculated spectra for an anisotropic s -wave pairing potential with uniaxial symmetry. (d) Calculated spectra for an anisotropic s -wave pairing potential with 4-fold in-plane modulation.

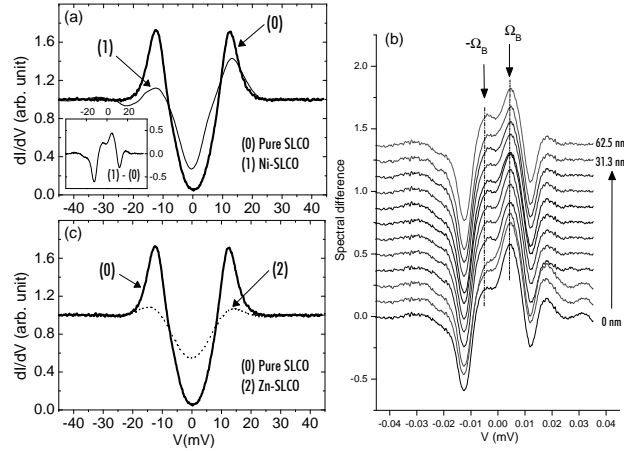


Fig. 3. (a) Comparison of the quasiparticle tunneling spectra of $\text{Sr}_{0.9}\text{La}_{0.1}\text{CuO}_2$ and $\text{Sr}_{0.9}\text{La}_{0.1}(\text{Cu}_{0.99}\text{Ni}_{0.01})\text{O}_2$ at $T = 4.2$ K. (b) Similar comparison for $\text{Sr}_{0.9}\text{La}_{0.1}\text{CuO}_2$ and $\text{Sr}_{0.9}\text{La}_{0.1}(\text{Cu}_{0.99}\text{Zn}_{0.01})\text{O}_2$. (c) Spectral difference due to Ni-impurities, showing long-range impurity bound states at $\pm\Omega_B$, similar to the Shiba impurity bands.

Scanning Tunneling Spectroscopic Studies of Cuprate Superconductors

reversal symmetry, as shown in Fig. 3(a). In contrast, 1 % Zn-isubstitutions result in significant disorder states without reduction in either the superconducting gap (Fig. 3(b)) or T_c .

The inset of Fig. 3(a) illustrates the spectral contribution due to Ni-impurities, and the corresponding gradual spatial evolution is shown in Fig. 3(c). Such impurity spectra are in contrast to the rapid spatial variations in (Zn,Mg)-substituted YBCO (see Fig. 1(c))⁴ and in Ni-substituted BSCCO.⁵⁰ The spectral contributions of Ni-impurities resemble the Shiba states for magnetic impurity bands in s -wave superconductors,⁴⁷ and the bound state energies are found to peak at $\pm\Omega_B$, where

$$|\Omega_B/\Delta_0| = (\pi/2)JSN_F \equiv \zeta. \quad (4)$$

Equation (4) clearly differs from Eq. (3), the latter being associated with magnetic impurities in d -wave superconductors. Using $\Omega_B \sim 5$ meV and $\Delta_0 \sim 13$ meV, we obtain $\zeta \sim 2/3$. The assumption of impurity bands can be justified by noting that the average Ni-Ni separation (~ 1.8 nm) is shorter than the in-plane superconducting coherence lengths of SLCO (~ 4.8 nm),⁴⁶ such that substantial overlap of impurity wavefunctions can be expected.

4. SUMMARY

Our STS studies of both p-type and n-type cuprates reveal that the pairing symmetry, pseudogap phenomenon and spin fluctuations are in fact not universal. The only ubiquitous features among all cuprates appear to be the strong electronic correlation and nearest-neighbor Cu^{2+} - Cu^{2+} antiferromagnetic interaction in the CuO_2 planes.

ACKNOWLEDGMENTS

This research is jointly supported by NSF grant DMR-0103045 at Caltech, by NASA at the Jet Propulsion Laboratory, by the Ministry of Science and Technology of Korea at the Pohang University, and by NEDO at SRL/ISTEC in Japan.

REFERENCES

1. S. Sachdev, *Science* **288**, 475 (2000); and references therein.
2. M. Vojta, Y. Zhang, and S. Sachdev, *Phys. Rev. B* **62** 6721 (2000).
3. D.-H. Lee, *Phys. Rev. Lett.* **88** 227003 (2002).

N.-C. Yeh *et al.*

4. N.-C. Yeh *et al.*, *Phys. Rev. Lett.* **87**, 087003 (2001).
5. N.-C. Yeh *et al.*, *Physica C* **364-365**, 450 (2001).
6. N.-C. Yeh *et al.*, *Physica C* **367**, 174 (2002).
7. C.-T. Chen *et al.*, *Phys. Rev. Lett.* **88**, 227002 (2002).
8. D.J. van Harlingen, *Rev. Mod. Phys.* **67**, 515 (1995).
9. C.-C. Tsuei and J. Kirtley, *Rev. Mod. Phys.* **72**, 969 (2000).
10. D. Pines, *Physica C* **282-287**, 273 (1997).
11. T. Timusk and B. Statt, *Rep. Prog. Phys.* **62**, 61 (1999).
12. V.J. Emery and S.A. Kivelson, *Nature* **374**, 434 (1995).
13. G. Siebold *et al.*, *Phys. Rev. B* **58**, 13506 (1998).
14. C.M. Varma, *Phys. Rev. B* **55**, 14554 (1997).
15. V.J. Emery, S.A. Kivelson, and O. Zachar, *Phys. Rev. B* **56**, 6120 (1997).
16. Y.J. Uemura *et al.*, *Phys. Rev. Lett.* **62**, 2317 (1989).
17. S. Chakravarty *et al.*, *Phys. Rev. B* **63**, 094503 (2001).
18. P.A. Lee and X.G. Wen, *Phys. Rev. Lett.* **78**, 4111 (1997).
19. J.Y.T. Wei *et al.*, *Physica B* **284**, 973 (2000).
20. R.P. Vasquez *et al.*, *Appl. Phys. Lett.* **53**, 2692 (1988).
21. R.P. Vasquez *et al.*, *J. Phys.: Condens. Matter* **13**, 7977 (2001).
22. J.Y.T. Wei *et al.*, *Phys. Rev. Lett.* **81**, 2542 (1998).
23. I. Maggio-Aprile *et al.*, *J. Electr. Spectro.* **109**, 147 (2000).
24. N. Miyakawa *et al.*, *Phys. Rev. Lett.* **83**, 1018 (1999); *ibid.* **80**, 157 (1998).
25. V.M. Krasnov *et al.*, *Phys. Rev. Lett.* **84**, 5860 (2000).
26. K.M. Lang *et al.*, *Nature* **415**, 412 (2002).
27. S. Misra *et al.*, *Phys. Rev. Lett.* **89**, (2002).
28. A.V. Balatsky, M.I. Salkola and A. Rosengren, *Phys. Rev. B* **51**, 15547 (1995).
29. M.I. Salkola *et al.*, *Phys. Rev. Lett.* **77**, 1841 (1996).
30. M.E. Flatte and J.M. Byers, *Phys. Rev. B* **56**, 11213 (1997).
31. M.I. Salkola, A.V. Balatsky and J.R. Schrieffer, *Phys. Rev. B* **55**, 12648 (1997).
32. M. Vojta and R. Bulla, *Phys. Rev. B* **65**, 014511 (2001).
33. H. Alloul *et al.*, *Phys. Rev. Lett.* **67**, 3140 (1991).
34. K. Ishida *et al.*, *Phys. Rev. Lett.* **76**, 531 (1996).
35. Y. Sidis *et al.*, *Phys. Rev. Lett.* **84**, 5900 (2000).
36. P.W. Anderson, *Phys. Rev. Lett.* **3**, 325 (1959).
37. A.V. Chubukov and N. Gemelke, *Phys. Rev. B* **61**, R6467 (2000).
38. C.-L. Wu, C.-Y. Mou, and D. Chang, *Phys. Rev. B* **63**, 172503 (2001).
39. A. Lanzara *et al.*, *Nature* **412**, 510 (2001).
40. J.X. Zhu, C.S. Ting and C.R. Hu, *Phys. Rev. B* **62**, 6027 (2000).
41. S.H. Pan *et al.*, *Nature* **403**, 746 (2000).
42. L. Alff *et al.*, *Phys. Rev. Lett.* **83**, 2644 (1999).
43. C.-C. Tsuei and J. Kirtley, *Phys. Rev. Lett.* **72**, 969 (2000).
44. J.A. Skinta *et al.*, *Phys. Rev. Lett.* **88**, 207005 (2002).
45. A.A. Abrikosov and L.P. Gor'kov, *Soviet Phys. JETP* **12**, 1243 (1961).
46. C.U. Jung *et al.*, *Physica C* **366**, 299 (2002).
47. H. Shiba, *Prog. Theor. Phys.* **40**, 435 (1968).
48. L. Alff, private communications.
49. C.U. Jung *et al.*, *Phys. Rev. B* **65**, 172501 (2002).
50. E.W. Hudson *et al.*, *Nature* **411**, 922 (2001).